Acta Cryst C STRUCTURAL CHEMISTRY

ISSN 2053-2296

Single-crystal structure of the spicy capsaicin

Matic Lozinšek*

Jožef Stefan Institute, Jamova cesta 39, 1000 Ljubljana, Slovenia. *Correspondence e-mail: matic.lozinsek@ijs.si

Received 3 January 2025
Accepted 23 February 2025

Edited by S. Moggach, The University of Western Australia, Australia

Keywords: capsaicin; capsaicinoid; *Capsicum*; crystal structure; single-crystal X-ray diffraction; natural product.

CCDC reference: 2426261

Supporting information: this article has supporting information at journals.iucr.org/c

The crystal structure of capsaicin ($C_{18}H_{27}NO_3$), or *trans*-8-methyl-*N*-vanillylnon-6-enamide, the natural product responsible for the spiciness of chilli peppers, was determined using low-temperature single-crystal X-ray diffraction. The reported crystal structure is in good agreement with previous determinations based on powder X-ray diffraction data. The localization and free refinement of all H atoms revealed that each capsaicin molecule is hydrogen bonded to four other molecules, with the O—H and N—H groups acting as hydrogen-bond donors, and the C=O group serving as a bifurcated hydrogen-bond acceptor.

1. Introduction

Capsaicin (Scheme 1) [systematic name (*E*)-*N*-[(4-hydroxy-3-methoxyphenyl)methyl]-8-methylnon-6-enamide; CAS: 404-86-4] is the principal bioactive compound from the capsaicinoid family of secondary metabolites found in the fruits of chilli pepper plants, which belong to the genus *Capsicum* with a very rich diversity of cultivars (Fig. 1). This natural product is primarily responsible for the spiciness or the heat sensation of hot chillies and acts as a potent agonist of the TRPV1 (transient receptor potential vanilloid 1) heat receptor, eliciting the characteristic burning sensation and making it a strong irritant (Caterina *et al.*, 1997). Chilli peppers have been cultivated for several millennia and are integral to the culinary traditions of many cultures worldwide, with their consumption and popularity continuing to rise (Spence, 2018; Bosland & Votava, 2012). Beyond their culinary use, capsaicin and capsaicinoids have garnered attention for their pharmacological properties and diverse biological activity (Srinivasan, 2016; Spence, 2018). The pungency of chillies is quantified using the Scoville Heat Scale, where capsaicin is assigned a value of 16 million Scoville Heat Units (SHU), reflecting its extreme potency (Scoville, 1912; Collins *et al.*, 1995; Bosland & Votava, 2012). Its unique physiological effects and diverse applications have made capsaicin a subject of extensive research.

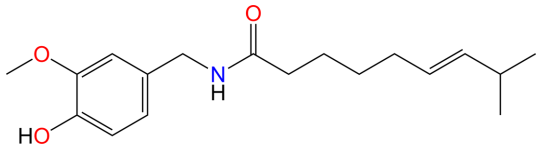

Scheme 1

The Cambridge Structural Database (CSD, Version 5.46, November 2024; Groom *et al.*, 2016) contains two previous structure determinations of the capsaicin crystal structure. The oldest entry, with CSD refcode FABVAF (Oliver, 1985), reports only the unit-cell parameters, without atomic coordinates. The second entry, FABVAF01, is a structure determi-

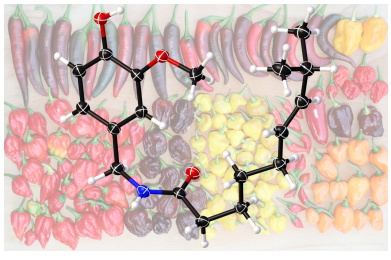

Figure 1
A colourful variety of capsaicin-containing spicy chilli pepper fruits (*Capsicum*).

nation based on synchrotron powder X-ray diffraction (PXRD) data employing simulated annealing (David *et al.*, 1998); however, the atomic coordinates were not refined, as the model of the capsaicin molecule was constructed using standard bond lengths and angles. The report mentions a single-crystal structure determination, which was used to validate the simulated annealing solution, but the single-crystal data were neither published nor deposited in the CSD. Similarly, unpublished single-crystal data were also used as a reference crystal structure for another structure redetermination of capsaicin *via* a simulated annealing approach from laboratory monochromatic capillary transmission PXRD data (Florence *et al.*, 2005).[1] Capsaicin has also been employed as a test sample in structure determination from powder diffraction data (Shankland *et al.*, 2013), utilizing a hybrid Monte Carlo method (Markvardsen *et al.*, 2005) and a local minimization approach (Shankland *et al.*, 2010). Furthermore, the crystal structure of an α-fluorinated capsaicin derivative (FOSXOB; Winkler *et al.*, 2009) and a cocrystal of a zinc coordination complex with a disordered capsaicin guest molecule (SOLZOM; Orton & Coles, 2024) were reported. The Protein Data Bank (PDB; Berman *et al.*, 2000) contains several experimentally determined structures of macromolecular complexes with capsaicin (PDB entry 4dy) as a ligand, including 7vek (Maharjan *et al.*, 2022), 7lr0 (Nadezhdin *et al.*, 2021), 7lpa, 7lpb, 7lpd and 7lpe (Kwon *et al.*, 2021), as well as 2n27 (Hetényi *et al.*, 2016).

The PXRD crystal structure of capsaicin (David *et al.*, 1998) has frequently served as a starting point for calculations and as a benchmark in computational studies (Alberti *et al.*, 2008; Siudem *et al.*, 2017; Soriano-Correa *et al.*, 2023).

Single-crystal X-ray diffraction (SCXRD) is considered a 'gold standard' (Bond, 2014) for the structural elucidation of natural products and continues to provide valuable insights into the crystal structures of naturally occurring crystals, with recent examples of such studies including (+)-cedrol hemihydrate (Chakoumakos & Wang, 2024) and calcium (2*R*,3*R*)-tartrate tetrahydrate (Polo *et al.*, 2024). Increasingly, 3D electron diffraction is gaining prominence in natural product characterization (Delgadillo *et al.*, 2024), because it enables crystal structure and absolute configuration determination on nanometer-sized crystallites, as demonstrated by recent studies of beauveriolide I (Gurung *et al.*, 2024) and berkecoumarin (Decato *et al.*, 2024).

In this work, the crystal structure of capsaicin was determined using low-temperature single-crystal X-ray diffraction, providing a detailed insight into its molecular geometry, conformation and hydrogen-bonding interactions.

Table 1
Experimental details.

Crystal data	
Chemical formula	$C_{18}H_{27}NO_3$
M_r	305.40
Crystal system, space group	Monoclinic, $P2_1/c$
Temperature (K)	100
a, b, c (Å)	12.2165 (3), 14.7791 (4), 9.4719 (2)
β (°)	94.035 (2)
V (Å^3)	1705.89 (8)
Z	4
Radiation type	Cu $K\alpha$
μ (mm^{-1})	0.64
Crystal size (mm)	0.08 × 0.06 × 0.03
Data collection	
Diffractometer	Rigaku XtaLAB Synergy-S Dualflex diffractometer with an Eiger2 R CdTe 1M detector
Absorption correction	Multi-scan (*CrysAlis PRO*; Rigaku OD, 2024)
T_{min}, T_{max}	0.683, 1.000
No. of measured, independent and observed [$I > 2\sigma(I)$] reflections	18993, 3508, 2644
R_{int}	0.054
(sin $\theta/\lambda)_{max}$ (Å^{-1})	0.630
Refinement	
$R[F^2 > 2\sigma(F^2)]$, $wR(F^2)$, S	0.044, 0.112, 1.04
No. of reflections	3508
No. of parameters	307
H-atom treatment	All H-atom parameters refined
$\Delta\rho_{max}$, $\Delta\rho_{min}$ (e Å^{-3})	0.20, −0.21

Computer programs: *CrysAlis PRO* (Rigaku OD, 2024), *SUPERFLIP* (Palatinus & Chapuis, 2007; Palatinus & van der Lee, 2008; Palatinus *et al.*, 2012), *SHELXL2019* (Sheldrick, 2015), *DIAMOND* (Brandenburg, 2018), *OLEX2* (Dolomanov *et al.*, 2009), *Mercury* (Macrae *et al.*, 2020) and *publCIF* (Westrip, 2010).

2. Experimental

2.1. Single-crystal selection

Capsaicin is a potent irritant and, to minimize exposure to the sample, it was handled as though the compound were air sensitive (Motaln *et al.*, 2024). The sample of capsaicin was procured from a commercial source (Sigma–Aldrich, ≥95%) and stored in a refrigerator within a nitrogen-filled glovebox (Vigor SG1200/750E). A small amount of the microcrystalline powder was transferred onto a thin layer of Baysilone-Paste (Bayer-Silicone, mittelviskos) on a watch glass inside the glovebox and covered with a layer of perfluorodecaline

[1] In both articles (David *et al.*, 1998; Florence *et al.*, 2005), the unpublished single-crystal data of capsaicin is credited to C. S. Frampton.

Table 2
Comparison of the unit-cell parameters of capsaicin crystal structures derived from previous structural determinations and the present work.

CSD refcode	FABVAF	FABVAF01	–	–	–
Reference	Oliver (1985)	David *et al.* (1998)	Florence *et al.* (2005)	Shankland *et al.* (2010)	This work
Space group	$P2_1/c$	$P2_1/c$	$P2_1/c$	$P2_1/c$	$P2_1/c$
a (Å)	12.380 (4)	12.2234 (1)	12.672	12.224	12.2165 (3)
b (Å)	14.814 (8)	14.7900 (1)	14.980	14.787	14.7791 (4)
c (Å)	9.491 (3)	9.4691 (1)	9.426	9.468	9.4719 (2)
β (°)	93.63 (3)	93.9754 (3)	93.69	93.972	94.035 (2)
V (Å^3)	1737.13	1707.30	1785.6	1707.3	1705.89 (8)
T (K)	173	100	Room temperature	100	100

(Fluorochem, 96.0%). A small crystal, measuring 27 µm × 63 µm × 75 µm, was selected under a polarizing microscope and attached to a MiTeGen Dual-Thickness MicroLoop using the Baysilone-Paste.

2.2. X-ray data collection and processing

Low-temperature single-crystal X-ray diffraction data were collected using a Rigaku OD XtaLAB Synergy-S instrument equipped with PhotonJet Ag and Cu microfocus X-ray tubes, a Dectris EIGER2 R CdTe 1M hybrid photon-counting detector and an Oxford Cryosystems Cryostream 800 Plus sample cooler. The crystal was measured at 100 K using Cu $K\alpha$ radiation (λ = 1.54184 Å). Experimental details on crystal data, data collection, and structure refinement are summarized in Table 1. *CrysAlis PRO* software (Rigaku OD, 2024) was used for data collection and reduction, and the crystal structure was solved and refined within the *OLEX2* program (Dolomanov *et al.*, 2009) using *SUPERFLIP* (Palatinus & Chapuis, 2007; Palatinus & van der Lee, 2008; Palatinus *et al.*, 2012) and *SHELXL* (Sheldrick, 2015), respectively. The measured crystal was an aggregate with two components; however, due to the presence of only a small fraction of overlapped reflections (<5%), data integration was performed on the major component (Bear *et al.*, 2023). The positions and isotropic displacement parameters (U_{iso}) of all H atoms were refined freely (Cooper *et al.*, 2010). Molecular graphics were generated using *DIAMOND* (Brandenburg, 2018).

3. Results and discussion

Capsaicin crystallizes in the monoclinic space group $P2_1/c$, with one molecule in the asymmetric unit (Fig. 2) and four molecules in the unit cell (Table 1). The unit-cell parameters determined at 100 K in this study are in good agreement with those obtained previously by powder X-ray diffraction at 100 K (David *et al.*, 1998; Shankland *et al.*, 2010) (Table 2), with observed differences smaller than 0.1%. Similarly, the conformation of the capsaicin molecule observed in the present SCXRD determination and the previous PXRD determination (David *et al.*, 1998) are very similar, with root-mean-square deviations (RMSDs) for their alignment of 0.162 and 0.276 Å calculated in *Mercury* (Macrae *et al.*, 2020) and *OLEX2* (Dolomanov *et al.*, 2009), respectively. The most notable conformational differences involve the positions of H atoms and specific C atoms, namely, C11, C12, C15 and C18, which are displaced by 0.31, 0.21, 0.36 and 0.27 Å, respectively (Fig. 3).

In contrast to the typical representation of the capsaicin molecule (Scheme 1), where the 8-methylnon-6-enamide side

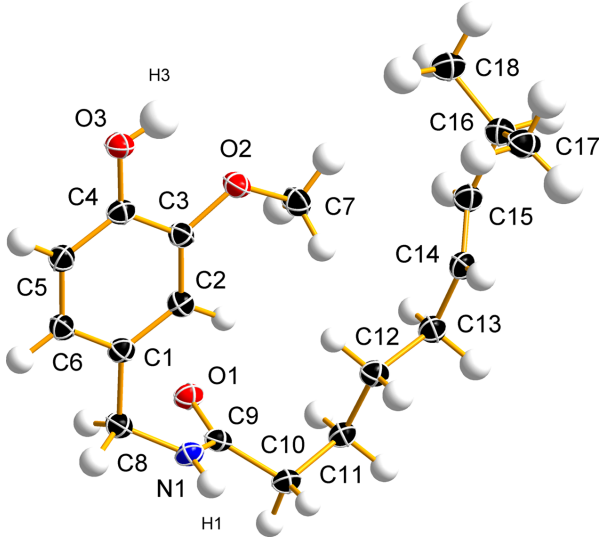

Figure 2
The asymmetric unit and selected atom labels of the capsaicin crystal structure, with displacement ellipsoids plotted at the 50% probability level.

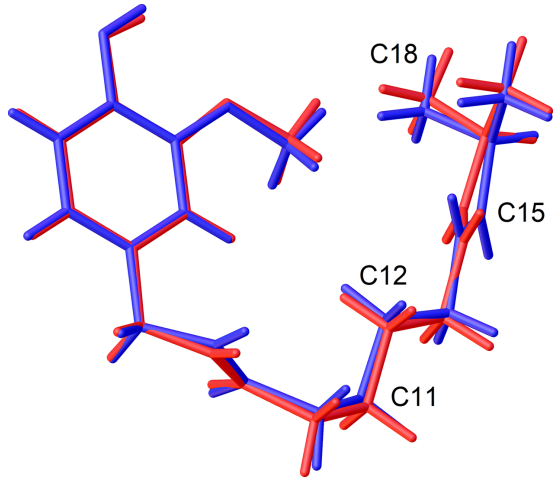

Figure 3
Molecular overlap comparison of capsaicin molecular conformations from SCXRD crystal structure determination (red; this work) and PXRD simulated annealing (blue; David *et al.*, 1998).

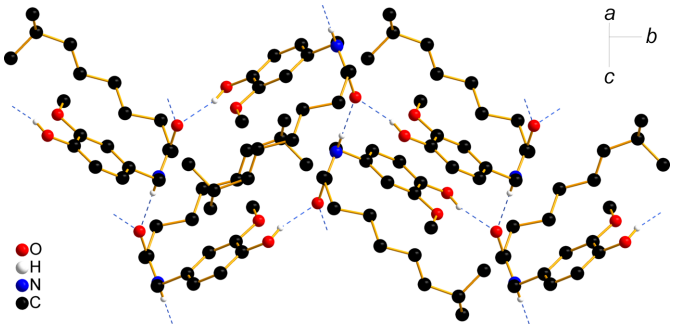

Figure 4
Hydrogen-bonding motifs in the crystal structure of capsaicin. H atoms not involved in hydrogen bonding have been omitted for clarity.

chain is depicted pointing away from the benzene ring, the crystal structure reveals that it bends back towards the vanillyl group and lies roughly parallel to the plane of the ring (Fig. 2). Atoms C15 and C16 are positioned 0.913 (5) and 0.612 (6) Å above the benzene-ring plane, respectively. The H16—C16—C15—H15 torsion angle is −66.4 (18)°, placing atom C17 0.825 (6) Å below and atom C18 1.578 (6) Å above the benzene-ring plane. The OH group is oriented parallel to the arene ring, while the methyl group (C7) is displaced by 0.109 (3) Å from the plane of the benzene ring. The dihedral angle between the plane of the amide group [–(O═)CNH–] and that of the benzene ring is 75.9 (4)°. The length of the C═C double bond, which adopts a *trans* configuration, is 1.325 (2) Å. Bond distances involving heteroatom functional groups [C—OH = 1.363 (2) Å, C—OCH_3 = 1.369 (2) Å, O—CH_3 = 1.423 (2) Å, C═O = 1.2459 (19) Å, N—CO = 1.334 (2) Å and N—CH_2 = 1.452 (2) Å] are within the expected ranges (Allen *et al.*, 1987).

In the crystal structure, each capsaicin molecule forms hydrogen bonds with four others, with the O—H and N—H groups functioning as hydrogen-bond donors and the C═O group acting as a bifurcated hydrogen-bond acceptor (Table 3). The resulting conjoined tetrameric hydrogen-bonded rings, described by graph-set notations $R_4^2(20)$ and $R_4^4(28)$ (Etter, 1990) (Fig. 4), link the capsaicin molecules into a double layer with a herringbone pattern extending within the *bc* plane (Fig. 5). The distance between the benzene-ring planes of neighbouring stacked molecules is 3.370 (3) Å in the smaller hydrogen-bonded ring and 4.671 (5) Å in the larger one. The double layers, with the hydrogen-bonded vanillyl and amide groups at the centre and the alkenyl chains on the exterior, are stacked along the crystallographic *a* direction (Fig. 5).

Table 3
Hydrogen-bond geometry (Å, °).

D—H···*A*	*D*—H	H···*A*	*D*···*A*	*D*—H···*A*
O3—H3···O1^{i}	0.88 (3)	1.93 (3)	2.7621 (17)	158 (2)
N1—H1···O1^{ii}	0.85 (2)	2.13 (2)	2.9769 (18)	175.7 (19)

Symmetry codes: (i) $-x+1, y+\frac{1}{2}, -z+\frac{1}{2}$; (ii) $x, -y+\frac{1}{2}, z-\frac{1}{2}$.

4. Conclusion

A low-temperature single-crystal X-ray diffraction study of capsaicin, the natural product responsible for the pungency of chilli peppers, was reported for the first time. The determined crystal structure aligns well with the previous simulated annealing structure solution based on powder X-ray diffraction data. In the present model, all H atoms were precisely localized and refined freely, enabling an accurate description of the hydrogen-bonding interactions. Each capsaicin molecule forms hydrogen bonds with four other molecules, with the O—H and N—H groups acting as hydrogen-bond donors, and the C═O group serving as a bifurcated hydrogen-bond acceptor, resulting in the formation of double layers.

Acknowledgements

The author is grateful to Assistant Professor Mirela Dragomir for inspiring his enthusiasm for chilli cultivation and spicy food.

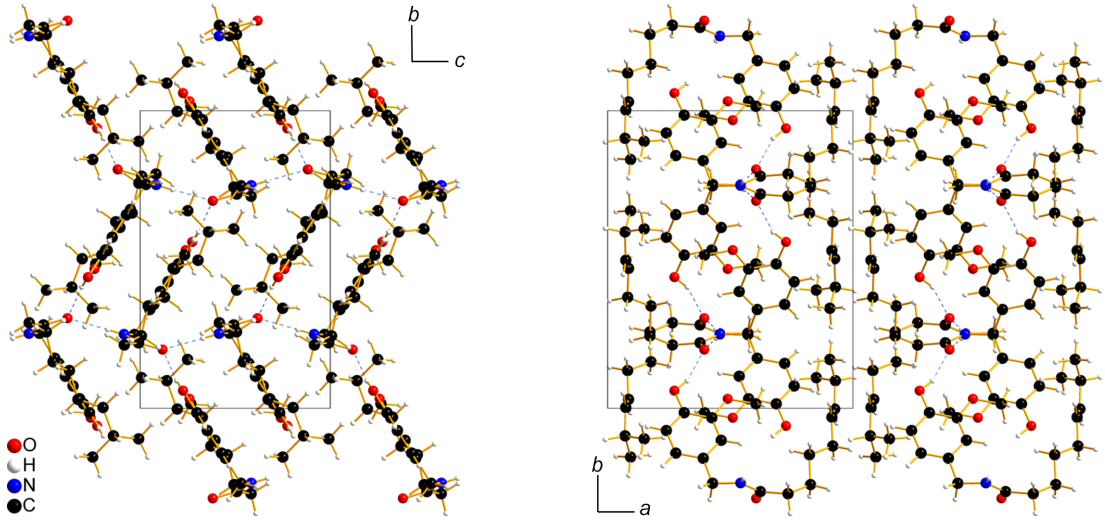

Figure 5
Packing diagrams and the unit cell of the capsaicin crystal structure viewed along the crystallographic *a* axis (left) and the crystallographic *c* axis (right).

Funding information

Funding for this research was provided by: European Research Council (ERC) under the European Union's Horizon 2020 Research and Innovation Programme (grant No. 950625); Jožef Stefan Institute Director's Fund.

References

Alberti, A., Galasso, V., Kovač, B., Modelli, A. & Pichierri, F. (2008). *J. Phys. Chem. A*, **112**, 5700–5711.
Allen, F. H., Kennard, O., Watson, D. G., Brammer, L., Orpen, A. G. & Taylor, R. (1987). *J. Chem. Soc. Perkin Trans. 2*, pp. S1–S19.
Bear, J. C., Terzoudis, N. & Cockcroft, J. K. (2023). *IUCrJ*, **10**, 720–728.
Berman, H. M., Westbrook, J., Feng, Z., Gilliland, G., Bhat, T. N., Weissig, H., Shindyalov, I. N. & Bourne, P. E. (2000). *Nucleic Acids Res.* **28**, 235–242.
Bond, A. D. (2014). *Resonance*, **19**, 1087–1092.
Bosland, P. W. & Votava, E. J. (2012). *Peppers: Vegetable and Spice Capsicums*, 2nd ed., *Crop Production Science in Horticulture Series*. Cambridge, MA, USA: CABI.
Brandenburg, K. (2018). *DIAMOND*. Crystal Impact GbR, Bonn, Germany.
Caterina, M. J., Schumacher, M. A., Tominaga, M., Rosen, T. A., Levine, J. D. & Julius, D. (1997). *Nature*, **389**, 816–824.
Chakoumakos, B. C. & Wang, X. (2024). *Acta Cryst.* C**80**, 43–48.
Collins, M. D., Wasmund Mayer, L. & Bosland, P. W. (1995). *HortScience*, **30**, 137–139.
Cooper, R. I., Thompson, A. L. & Watkin, D. J. (2010). *J. Appl. Cryst.* **43**, 1100–1107.
David, W. I. F., Shankland, K. & Shankland, N. (1998). *Chem. Commun.* pp. 931–932.
Decato, D., Palatinus, L., Stierle, A. & Stierle, D. (2024). *Acta Cryst.* C**80**, 143–147.
Delgadillo, D. A., Burch, J. E., Kim, L. J., de Moraes, L. S., Niwa, K., Williams, J., Tang, M. J., Lavallo, V. G., Khatri Chhetri, B., Jones, C. G., Hernandez Rodriguez, I., Signore, J. A., Marquez, L., Bhanushali, R., Woo, S., Kubanek, J., Quave, C., Tang, Y. & Nelson, H. M. (2024). *ACS Cent. Sci.* **10**, 176–183.
Dolomanov, O. V., Bourhis, L. J., Gildea, R. J., Howard, J. A. K. & Puschmann, H. (2009). *J. Appl. Cryst.* **42**, 339–341.
Etter, M. C. (1990). *Acc. Chem. Res.* **23**, 120–126.
Florence, A. J., Shankland, N., Shankland, K., David, W. I. F., Pidcock, E., Xu, X., Johnston, A., Kennedy, A. R., Cox, P. J., Evans, J. S. O., Steele, G., Cosgrove, S. D. & Frampton, C. S. (2005). *J. Appl. Cryst.* **38**, 249–259.
Groom, C. R., Bruno, I. J., Lightfoot, M. P. & Ward, S. C. (2016). *Acta Cryst.* B**72**, 171–179.
Gurung, K., Šimek, P., Jegorov Jr, A. & Palatinus, L. (2024). *Acta Cryst.* C**80**, 56–61.
Hetényi, A., Németh, L., Wéber, E., Szakonyi, G., Winter, Z., Jósvay, K., Bartus, E., Oláh, Z. & Martinek, T. A. (2016). *FEBS Lett.* **590**, 2768–2775.
Kwon, D. H., Zhang, F., Suo, Y., Bouvette, J., Borgnia, M. J. & Lee, S.-Y. (2021). *Nat. Struct. Mol. Biol.* **28**, 554–563.
Macrae, C. F., Sovago, I., Cottrell, S. J., Galek, P. T. A., McCabe, P., Pidcock, E., Platings, M., Shields, G. P., Stevens, J. S., Towler, M. & Wood, P. A. (2020). *J. Appl. Cryst.* **53**, 226–235.
Maharjan, R., Fukuda, Y., Nakayama, T., Nakayama, T., Hamada, H., Ozaki, S.-i. & Inoue, T. (2022). *Acta Cryst.* D**78**, 379–389.
Markvardsen, A. J., Shankland, K., David, W. I. F. & Didlick, G. (2005). *J. Appl. Cryst.* **38**, 107–111.
Motaln, K., Gurung, K., Brázda, P., Kokalj, A., Radan, K., Dragomir, M., Žemva, B., Palatinus, L. & Lozinšek, M. (2024). *ACS Cent. Sci.* **10**, 1733–1741.
Nadezhdin, K. D., Neuberger, A., Nikolaev, Y. A., Murphy, L. A., Gracheva, E. O., Bagriantsev, S. N. & Sobolevsky, A. I. (2021). *Nat. Commun.* **12**, 2154.
Oliver, J. D. (1985). *Am. Crystallogr. Assoc. Abstr. Pap. (Winter)*, **13**, 57.
Orton, J. B. & Coles, S. J. (2024). *CSD Communication*, CCDC 2339733, https://dx.doi.org/10.5517/ccdc.csd.cc2jjp81.
Palatinus, L. & Chapuis, G. (2007). *J. Appl. Cryst.* **40**, 786–790.
Palatinus, L., Prathapa, S. J. & van Smaalen, S. (2012). *J. Appl. Cryst.* **45**, 575–580.
Palatinus, L. & van der Lee, A. (2008). *J. Appl. Cryst.* **41**, 975–984.
Polo, A., Soriano-Jarabo, A., Rodríguez, R., Macías, R., García-Orduña, P. & Sanz Miguel, P. J. (2024). *Acta Cryst.* C**80**, 681–684.
Rigaku OD (2024). *CrysAlis PRO*. Rigaku Corporation, Wrocław, Poland.
Scoville, W. L. (1912). *J. Am. Pharm. Assoc.* **1**, 453–454.
Shankland, K., Markvardsen, A. J., Rowlatt, C., Shankland, N. & David, W. I. F. (2010). *J. Appl. Cryst.* **43**, 401–406.
Shankland, K., Spillman, M. J., Kabova, E. A., Edgeley, D. S. & Shankland, N. (2013). *Acta Cryst.* C**69**, 1251–1259.
Sheldrick, G. M. (2015). *Acta Cryst.* C**71**, 3–8.
Siudem, P., Paradowska, K. & Bukowicki, J. (2017). *J. Mol. Struct.* **1146**, 773–781.
Soriano-Correa, C., Pérez de la Luz, A. & Sainz-Díaz, C. I. (2023). *J. Pharm. Sci.* **112**, 798–807.
Spence, C. (2018). *Int. J. Gastron. Food. Sci.* **12**, 16–21.
Srinivasan, K. (2016). *Crit. Rev. Food Sci. Nutr.* **56**, 1488–1500.
Westrip, S. P. (2010). *J. Appl. Cryst.* **43**, 920–925.
Winkler, M., Moraux, T., Khairy, H. A., Scott, R. H., Slawin, A. M. Z. & O'Hagan, D. (2009). *ChemBioChem*, **10**, 823–828.

supporting information

Acta Cryst. (2025). C**81**, 188-192 [https://doi.org/10.1107/S2053229625001706]

Single-crystal structure of the spicy capsaicin

Matic Lozinšek

Computing details

(6*E*)-*N*-[(4-Hydroxy-3-methoxyphenyl)methyl]-8-methylnon-6-enamide

Crystal data

$C_{18}H_{27}NO_3$
$M_r = 305.40$
Monoclinic, $P2_1/c$
$a = 12.2165$ (3) Å
$b = 14.7791$ (4) Å
$c = 9.4719$ (2) Å
$\beta = 94.035$ (2)°
$V = 1705.89$ (8) Å^3
$Z = 4$
$F(000) = 664$
$D_x = 1.189$ Mg m^{-3}
Cu $K\alpha$ radiation, $\lambda = 1.54184$ Å
Cell parameters from 5220 reflections
$\theta = 3.6$–$73.0°$
$\mu = 0.64$ mm^{-1}
$T = 100$ K
Plank, colourless
0.08 × 0.06 × 0.03 mm

Data collection

Rigaku XtaLAB Synergy-S Dualflex diffractometer with an Eiger2 R CdTe 1M detector
Radiation source: micro-focus sealed X-ray tube, PhotonJet (Cu) X-ray Source
Mirror monochromator
Detector resolution: 13.3333 pixels mm^{-1}
ω scans
Absorption correction: multi-scan (CrysAlis PRO; Rigaku OD, 2024)
$T_{min} = 0.683$, $T_{max} = 1.000$
18993 measured reflections
3508 independent reflections
2644 reflections with $I > 2\sigma(I)$
$R_{int} = 0.054$
$\theta_{max} = 76.1°$, $\theta_{min} = 3.6°$
$h = -15 \rightarrow 15$
$k = -18 \rightarrow 18$
$l = -11 \rightarrow 11$

Refinement

Refinement on F^2
Least-squares matrix: full
$R[F^2 > 2\sigma(F^2)] = 0.044$
$wR(F^2) = 0.112$
$S = 1.04$
3508 reflections
307 parameters
0 restraints
Primary atom site location: iterative
Hydrogen site location: difference Fourier map
All H-atom parameters refined
$w = 1/[\sigma^2(F_o^2) + (0.0432P)^2 + 0.8148P]$ where $P = (F_o^2 + 2F_c^2)/3$
$(\Delta/\sigma)_{max} < 0.001$
$\Delta\rho_{max} = 0.20$ e Å^{-3}
$\Delta\rho_{min} = -0.21$ e Å^{-3}

Special details

Geometry. All esds (except the esd in the dihedral angle between two l.s. planes) are estimated using the full covariance matrix. The cell esds are taken into account individually in the estimation of esds in distances, angles and torsion angles; correlations between esds in cell parameters are only used when they are defined by crystal symmetry. An approximate (isotropic) treatment of cell esds is used for estimating esds involving l.s. planes.

Fractional atomic coordinates and isotropic or equivalent isotropic displacement parameters (Å²)

	x	*y*	*z*	U_{iso}*/U_{eq}
O1	0.39422 (10)	0.19720 (8)	0.11809 (11)	0.0254 (3)
O2	0.51027 (10)	0.53170 (8)	0.24005 (13)	0.0286 (3)
O3	0.72757 (11)	0.55919 (9)	0.27416 (13)	0.0287 (3)
H3	0.675 (2)	0.5923 (17)	0.307 (3)	0.055 (7)*
N1	0.45776 (12)	0.24880 (10)	−0.08461 (15)	0.0239 (3)
H1	0.4432 (16)	0.2648 (13)	−0.170 (2)	0.030 (5)*
C1	0.61015 (14)	0.33202 (11)	0.05079 (16)	0.0230 (4)
C2	0.53676 (14)	0.39235 (12)	0.10650 (17)	0.0242 (4)
H2	0.4577 (15)	0.3816 (12)	0.0934 (18)	0.022 (5)*
C3	0.57495 (14)	0.46809 (11)	0.18172 (16)	0.0234 (4)
C4	0.68774 (14)	0.48509 (11)	0.20185 (16)	0.0242 (4)
C5	0.76058 (15)	0.42518 (12)	0.14703 (18)	0.0262 (4)
H5	0.8374 (17)	0.4383 (13)	0.162 (2)	0.031 (5)*
C6	0.72194 (15)	0.34929 (12)	0.07186 (18)	0.0256 (4)
H6	0.7740 (15)	0.3072 (13)	0.033 (2)	0.028 (5)*
C7	0.39533 (15)	0.51494 (14)	0.2336 (2)	0.0306 (4)
H7A	0.3643 (16)	0.5112 (13)	0.134 (2)	0.029 (5)*
H7B	0.3647 (18)	0.5657 (15)	0.285 (2)	0.039 (6)*
H7C	0.3784 (18)	0.4561 (15)	0.286 (2)	0.041 (6)*
C8	0.57184 (14)	0.24788 (12)	−0.02999 (19)	0.0266 (4)
H8A	0.5821 (15)	0.1939 (14)	0.033 (2)	0.028 (5)*
H8B	0.6209 (16)	0.2371 (13)	−0.112 (2)	0.032 (5)*
C9	0.37700 (14)	0.21995 (11)	−0.00818 (16)	0.0225 (3)
C10	0.26436 (14)	0.21276 (12)	−0.08335 (17)	0.0248 (4)
H10A	0.2634 (15)	0.2476 (12)	−0.173 (2)	0.024 (5)*
H10B	0.2546 (15)	0.1468 (14)	−0.1093 (19)	0.027 (5)*
C11	0.17246 (14)	0.24340 (12)	0.00656 (17)	0.0245 (4)
H11A	0.1756 (15)	0.2051 (13)	0.096 (2)	0.030 (5)*
H11B	0.0976 (16)	0.2284 (13)	−0.045 (2)	0.029 (5)*
C12	0.17693 (15)	0.34386 (12)	0.04219 (18)	0.0258 (4)
H12A	0.1737 (16)	0.3802 (14)	−0.049 (2)	0.035 (5)*
H12B	0.2496 (15)	0.3574 (12)	0.0974 (19)	0.023 (5)*
C13	0.08175 (15)	0.37320 (12)	0.12808 (18)	0.0270 (4)
H13A	0.0773 (15)	0.3332 (13)	0.216 (2)	0.029 (5)*
H13B	0.0088 (17)	0.3620 (14)	0.067 (2)	0.036 (5)*
C14	0.08545 (15)	0.47018 (12)	0.17305 (18)	0.0279 (4)
H14	0.0938 (16)	0.5146 (14)	0.099 (2)	0.032 (5)*
C15	0.07414 (15)	0.49742 (13)	0.30448 (18)	0.0290 (4)
H15	0.0643 (18)	0.4499 (15)	0.380 (2)	0.045 (6)*
C16	0.07110 (16)	0.59276 (13)	0.35942 (19)	0.0314 (4)
H16	−0.0088 (18)	0.6049 (14)	0.390 (2)	0.039 (6)*
C17	0.0938 (2)	0.66396 (14)	0.2505 (2)	0.0379 (5)
H17A	0.035 (2)	0.6610 (16)	0.166 (3)	0.057 (7)*
H17B	0.1730 (19)	0.6554 (15)	0.216 (2)	0.045 (6)*
H17C	0.0873 (19)	0.7256 (17)	0.290 (3)	0.054 (7)*

C18	0.14915 (18)	0.60282 (14)	0.4923 (2)	0.0348 (4)
H18A	0.1382 (18)	0.5535 (15)	0.563 (2)	0.042 (6)*
H18B	0.229 (2)	0.5977 (16)	0.467 (2)	0.051 (7)*
H18C	0.1348 (18)	0.6639 (16)	0.541 (2)	0.046 (6)*

Atomic displacement parameters (Å²)

	U^{11}	U^{22}	U^{33}	U^{12}	U^{13}	U^{23}
O1	0.0313 (6)	0.0264 (6)	0.0184 (6)	−0.0004 (5)	0.0003 (5)	0.0020 (4)
O2	0.0257 (6)	0.0266 (6)	0.0338 (6)	0.0001 (5)	0.0039 (5)	−0.0086 (5)
O3	0.0286 (7)	0.0276 (7)	0.0297 (7)	−0.0017 (5)	0.0012 (5)	−0.0070 (5)
N1	0.0277 (8)	0.0280 (8)	0.0160 (7)	−0.0004 (6)	0.0011 (6)	0.0004 (6)
C1	0.0269 (9)	0.0241 (9)	0.0180 (7)	0.0010 (7)	0.0019 (6)	0.0011 (6)
C2	0.0238 (9)	0.0255 (9)	0.0232 (8)	−0.0013 (7)	0.0023 (7)	0.0004 (6)
C3	0.0260 (8)	0.0234 (9)	0.0210 (8)	0.0025 (7)	0.0035 (6)	−0.0009 (6)
C4	0.0281 (9)	0.0239 (9)	0.0204 (8)	−0.0018 (7)	−0.0002 (6)	0.0007 (6)
C5	0.0245 (9)	0.0299 (9)	0.0240 (8)	0.0018 (7)	0.0004 (7)	0.0004 (7)
C6	0.0274 (9)	0.0267 (9)	0.0226 (8)	0.0045 (7)	0.0023 (7)	−0.0001 (7)
C7	0.0254 (9)	0.0322 (10)	0.0349 (10)	0.0004 (8)	0.0068 (8)	−0.0055 (8)
C8	0.0276 (9)	0.0255 (9)	0.0269 (9)	0.0015 (7)	0.0033 (7)	−0.0034 (7)
C9	0.0304 (9)	0.0184 (8)	0.0188 (8)	0.0015 (7)	0.0024 (6)	−0.0017 (6)
C10	0.0285 (9)	0.0262 (9)	0.0194 (8)	−0.0014 (7)	0.0000 (7)	−0.0013 (7)
C11	0.0261 (9)	0.0264 (9)	0.0207 (8)	−0.0010 (7)	0.0002 (7)	0.0000 (7)
C12	0.0302 (9)	0.0241 (9)	0.0235 (8)	−0.0001 (7)	0.0030 (7)	0.0004 (7)
C13	0.0285 (9)	0.0296 (10)	0.0228 (8)	0.0020 (7)	0.0015 (7)	0.0011 (7)
C14	0.0304 (9)	0.0295 (10)	0.0237 (9)	0.0049 (8)	0.0001 (7)	0.0013 (7)
C15	0.0287 (9)	0.0338 (10)	0.0246 (9)	0.0013 (8)	0.0021 (7)	0.0000 (7)
C16	0.0334 (10)	0.0337 (10)	0.0271 (9)	0.0035 (8)	0.0023 (8)	−0.0027 (7)
C17	0.0545 (14)	0.0304 (10)	0.0281 (10)	0.0075 (9)	−0.0023 (9)	−0.0010 (8)
C18	0.0423 (12)	0.0357 (11)	0.0260 (9)	−0.0024 (9)	0.0008 (8)	−0.0015 (8)

Geometric parameters (Å, º)

O1—C9	1.2459 (19)	C10—H10B	1.01 (2)
O2—C3	1.369 (2)	C10—C11	1.525 (2)
O2—C7	1.423 (2)	C11—H11A	1.02 (2)
O3—H3	0.88 (3)	C11—H11B	1.03 (2)
O3—C4	1.363 (2)	C11—C12	1.523 (2)
N1—H1	0.85 (2)	C12—H12A	1.01 (2)
N1—C8	1.452 (2)	C12—H12B	1.018 (19)
N1—C9	1.334 (2)	C12—C13	1.528 (2)
C1—C2	1.394 (2)	C13—H13A	1.03 (2)
C1—C6	1.390 (2)	C13—H13B	1.04 (2)
C1—C8	1.517 (2)	C13—C14	1.495 (3)
C2—H2	0.978 (18)	C14—H14	0.97 (2)
C2—C3	1.390 (2)	C14—C15	1.325 (2)
C3—C4	1.400 (2)	C15—H15	1.02 (2)
C4—C5	1.382 (2)	C15—C16	1.503 (3)

C5—H5	0.96 (2)	C16—H16	1.05 (2)
C5—C6	1.393 (2)	C16—C17	1.513 (3)
C6—H6	0.98 (2)	C16—C18	1.531 (3)
C7—H7A	1.00 (2)	C17—H17A	1.04 (3)
C7—H7B	0.98 (2)	C17—H17B	1.05 (2)
C7—H7C	1.03 (2)	C17—H17C	0.99 (3)
C8—H8A	1.00 (2)	C18—H18A	1.01 (2)
C8—H8B	1.02 (2)	C18—H18B	1.03 (2)
C9—C10	1.508 (2)	C18—H18C	1.03 (2)
C10—H10A	0.991 (19)		

C3—O2—C7	117.32 (13)	C11—C10—H10B	110.1 (11)
C4—O3—H3	112.4 (17)	C10—C11—H11A	108.3 (11)
C8—N1—H1	118.3 (13)	C10—C11—H11B	109.8 (11)
C9—N1—H1	119.5 (14)	H11A—C11—H11B	104.6 (15)
C9—N1—C8	122.11 (14)	C12—C11—C10	113.39 (14)
C2—C1—C8	122.10 (15)	C12—C11—H11A	111.1 (11)
C6—C1—C2	118.67 (16)	C12—C11—H11B	109.3 (11)
C6—C1—C8	119.23 (15)	C11—C12—H12A	109.3 (12)
C1—C2—H2	120.2 (11)	C11—C12—H12B	108.8 (10)
C3—C2—C1	120.50 (16)	C11—C12—C13	112.20 (15)
C3—C2—H2	119.3 (11)	H12A—C12—H12B	108.2 (15)
O2—C3—C2	125.27 (15)	C13—C12—H12A	108.5 (12)
O2—C3—C4	114.34 (14)	C13—C12—H12B	109.8 (10)
C2—C3—C4	120.39 (15)	C12—C13—H13A	110.9 (11)
O3—C4—C3	121.71 (15)	C12—C13—H13B	108.2 (11)
O3—C4—C5	119.13 (15)	H13A—C13—H13B	105.6 (15)
C5—C4—C3	119.16 (15)	C14—C13—C12	114.51 (15)
C4—C5—H5	117.6 (12)	C14—C13—H13A	108.7 (11)
C4—C5—C6	120.25 (16)	C14—C13—H13B	108.6 (11)
C6—C5—H5	122.1 (12)	C13—C14—H14	116.4 (12)
C1—C6—C5	121.03 (16)	C15—C14—C13	123.78 (17)
C1—C6—H6	119.0 (11)	C15—C14—H14	119.8 (12)
C5—C6—H6	119.9 (11)	C14—C15—H15	118.5 (13)
O2—C7—H7A	111.0 (11)	C14—C15—C16	128.08 (17)
O2—C7—H7B	104.7 (13)	C16—C15—H15	113.4 (12)
O2—C7—H7C	110.9 (12)	C15—C16—H16	107.5 (12)
H7A—C7—H7B	112.3 (17)	C15—C16—C17	113.94 (16)
H7A—C7—H7C	109.7 (16)	C15—C16—C18	110.26 (16)
H7B—C7—H7C	108.0 (17)	C17—C16—H16	106.5 (12)
N1—C8—C1	115.25 (14)	C17—C16—C18	111.06 (17)
N1—C8—H8A	107.3 (11)	C18—C16—H16	107.2 (11)
N1—C8—H8B	109.3 (11)	C16—C17—H17A	110.5 (14)
C1—C8—H8A	109.3 (11)	C16—C17—H17B	110.3 (12)
C1—C8—H8B	109.4 (11)	C16—C17—H17C	111.1 (14)
H8A—C8—H8B	105.9 (15)	H17A—C17—H17B	110.6 (18)
O1—C9—N1	121.73 (16)	H17A—C17—H17C	105.2 (19)
O1—C9—C10	121.40 (15)	H17B—C17—H17C	109.2 (18)

N1—C9—C10	116.84 (14)	C16—C18—H18A	111.9 (13)
C9—C10—H10A	108.8 (11)	C16—C18—H18B	110.5 (13)
C9—C10—H10B	105.7 (11)	C16—C18—H18C	109.7 (12)
C9—C10—C11	113.50 (14)	H18A—C18—H18B	105.9 (18)
H10A—C10—H10B	107.4 (15)	H18A—C18—H18C	107.5 (17)
C11—C10—H10A	111.0 (11)	H18B—C18—H18C	111.2 (18)
O1—C9—C10—C11	41.9 (2)	C7—O2—C3—C2	5.7 (2)
O2—C3—C4—O3	0.1 (2)	C7—O2—C3—C4	−175.03 (15)
O2—C3—C4—C5	−179.88 (14)	C8—N1—C9—O1	5.6 (2)
O3—C4—C5—C6	−179.54 (15)	C8—N1—C9—C10	−172.11 (14)
N1—C9—C10—C11	−140.32 (16)	C8—C1—C2—C3	179.07 (15)
C1—C2—C3—O2	179.62 (15)	C8—C1—C6—C5	−179.17 (15)
C1—C2—C3—C4	0.4 (2)	C9—N1—C8—C1	−88.2 (2)
C2—C1—C6—C5	0.0 (2)	C9—C10—C11—C12	65.51 (19)
C2—C1—C8—N1	19.0 (2)	C10—C11—C12—C13	178.09 (14)
C2—C3—C4—O3	179.46 (15)	C11—C12—C13—C14	176.74 (14)
C2—C3—C4—C5	−0.6 (2)	C12—C13—C14—C15	−130.33 (19)
C3—C4—C5—C6	0.5 (2)	C13—C14—C15—C16	−176.78 (17)
C4—C5—C6—C1	−0.2 (3)	C14—C15—C16—C17	−5.7 (3)
C6—C1—C2—C3	−0.1 (2)	C14—C15—C16—C18	−131.4 (2)
C6—C1—C8—N1	−161.81 (15)		

Hydrogen-bond geometry (Å, º)

D—H···*A*	*D*—H	H···*A*	*D*···*A*	*D*—H···*A*
O3—H3···O1^{i}	0.88 (3)	1.93 (3)	2.7621 (17)	158 (2)
N1—H1···O1^{ii}	0.85 (2)	2.13 (2)	2.9769 (18)	175.7 (19)

Symmetry codes: (i) −*x*+1, *y*+1/2, −*z*+1/2; (ii) *x*, −*y*+1/2, *z*−1/2.